



NTNU – Trondheim
Norwegian University of
Science and Technology

Python Framework for Design and Simulation of Integer-N ADPLLs

Cole Nielsen

Electronic Systems Design, Specialization Project

Submission date: December 2019

Supervisor: Trond Ytterdal, IET

Co-supervisor: Carsten Wulff, IET

Norwegian University of Science and Technology
Department of Electronic Systems

Abstract.

A pure-Python simulation and design automation framework for the design of integer-N all digital phase locked loop (ADPLL) frequency synthesizers is presented in this paper. The framework enables (a) automatic design of optimized discrete-time and quantized digital PLL loop filters, and (b) discrete-time simulation to verify filter and PLL designs for phase noise performance, lock-time and stability subject to variation using Monte-Carlo sampling. Simulation is performed with a discrete-event time domain simulator utilizing behavioral PLL component models, which permit accurate modeling effects of time-discretization and quantization in a ADPLL. Filter design automation is achieved via optimization of a prototype loop filter in a PLL for minimum total phase noise power and lock time, where lock time is maximally constrained. The optimizer utilizes continuous phase transfer function approximations of discrete PLL loop, allowing computationally fast estimates of phase noise and lock time. Thus continuous-to-discrete time conversion and coefficient quantization of the optimal filter is applied to yield a end loop-filter design. Second order optimization is utilized to minimize loop filter design error due to quantization effects.

Problem description.

To develop a standalone PLL simulation framework to aid and facilitate a later master's thesis project regarding the design of an all-digital, ultra-low power PLL (ULPPLL) frequency synthesizer. This framework is intended to address and ease all-digital PLL design and simulation challenges at a high level. Specifically it should allow for speedy PLL simulation defined with system and component-level specifications (e.g. desired frequency, gain of digitally controlled oscillator, phase detector resolution, divider modulus). This is to allow for development of component level specifications and validation of ideal PLL performance (phase noise, lock time, stability) before transistor level implementation. Furthermore, the framework should automate design of any pure-digital PLL components, namely loop-filter design, to accelerate overall time of PLL implementation.

Contents

1	Introduction	10
2	Theory	11
2.1	Continuous PLL Model	11
2.1.1	PLL Synthesizer architecture	12
2.1.2	Divider	12
2.1.3	Phase detector	12
2.1.4	Loop Filter	12
2.1.5	VCO	13
2.1.6	Continuous PLL Transfer function	13
2.1.7	PI-loop filter design	14
2.1.8	PI-controller peaking compensation	15
2.1.9	Alternative PID controller permutations	16
2.2	ADPLL - digital, discretized PLL Model	16
2.2.1	Divider	17
2.2.2	TDC	17
2.2.3	Loop Filter	18
2.2.4	DCO	19
2.2.5	Discrete-time PLL transfer function	20
2.3	ADPLL Noise Model	21
2.3.1	TDC noise	21
2.3.2	DCO noise	22
2.3.3	Divider noise	23
2.3.4	Loop filter noise - direct type I	24
2.3.5	PLL noise sensitivity transfer functions	25
2.3.6	PLL phase noise and output PSD relationship	26
2.3.7	PLL output-referred noise PSD	27
3	ADPLL Design Automation	27
3.1	Loop filter	28
3.2	Design sequence	28
4	Behavioral ADPLL simulation	28
4.1	Clock behavioral model	29
4.2	TDC behavioral model	29
4.3	Loop filter behavioral model	29
4.4	DCO behavioral model	30
4.5	Divider behavioral model	31
4.6	Post processing: lock time detection	31
4.7	Post processing: phase noise power spectrum estimate	31
4.8	Monte-Carlo sampling	32
5	Loop filter optimization	32
5.1	Fast estimation of PLL settling time	33
5.2	Estimation of PLL phase noise	34
5.3	Loop filter optimization algorithm	34
5.4	Loop filter optimization - finite word effects	35

6 Discussion and results	35
6.1 Divider noise constraint	36
6.2 Example exercise	37
7 Conclusion	37
8 Baseband phase noise in radio with PLL	37
8.1 Modulated Signal	38
8.2 Local oscillator - noisy PLL	38
8.3 Baseband phase noise	38
A Appendix - Schedule	41

List of Figures

1	Basic phase feedback network.	11
2	Basic PLL.	12
3	PI-controller PLL pole-zero locations.	14
4	Example PI-PLL responses with varied ζ	15
5	Basic ADPLL.	16
6	Digital divider signals.	17
7	TDC model.	18
8	Implementation of filter.	19
9	Discrete time PLL model.	20
10	TDC quantization noise models.	21
11	Quantization as via additive error signal.	21
12	DCO additive noise model.	22
13	Voltage to phase noise conversion.	22
14	Divider phase noise.	23
15	Direct type I filter implementation with quantization.	24
16	Full PLL additive noise model.	25
17	Simulation process.	28

List of Tables

1	System-level specifications	37
2	Component-level specifications.	37

Abbreviations.

ADPLL	All digital phase locked loop
BER	Bit error rate
BFGS	Broyden-Fletcher-Goldfarb-Shanno
BW	Bandwidth
CMOS	Complementary metal oxide semiconductor
DCO	Digitally controlled oscillator
DIV	Divider
DNL	Differential non-linearity
FFT	Fast Fourier transform
FM	Frequency modulation
FSK	Frequency shift keying
IF	Intermediate frequency
IIR	Infinite impulse response
ISM	Industrial scientific medicine
LF	Loop filter
LO	Local oscillator
LSB	Least significant bit
OTW	Oscillator tuning word
PD	Phase detector
PI	Proportional-integral
PID	Proportional-integral-derivative
PLL	Phase locked loop
PN	Phase noise
PSD	Power spectral density
PSK	Phase shift keying
RMS	Root mean squared
SNR	Signal to noise ratio
SSB	Single side band
TDC	Time to digital converter
TF	Transfer function
ULPPLL	Ultra low power phase locked loop
VCO	Voltage controlled oscillator

1 Introduction

Phase locked loops are extraordinarily useful frequency synthesizers that are vital to the operation of virtually all wired and wireless communication systems of today. The trend towards increasingly lower power wireless devices poses an acute need to reduce PLL power consumption. This is a challenge as PLLs typically rank among the highest power consuming components of a radio, and are necessarily so to limit phase noise. Reducing analog PLL power consumption can be a prohibitive challenge as the performance of analog loop filters degrade as a result of unavoidably lower charge pump current. However, recent CMOS process nodes with minimum gate lengths as small as 7nm allow for all-digital PLLs as an attractive alternative to analog designs due to low power consumption associated with the implementation of a digital loop filter. Digital loop-filters have a unique advantage where they can be scaled indefinitely as process nodes advance, while suffering no loss in performance.

All-digital PLLs introduce new challenges in the process of design in the ultra-low power domain. Low power design is complemented by low complexity design, which in a PLL transcribes to low resolution of phase detectors, digitally tunable oscillators, and loop filter digital data paths. In other words, effects of quantization are strong. Whereas analog designs and high power/resolution digital designs can be effectively analyzed (even by hand) with transfer functions in the Z-domain, time domain simulation is necessary to capture quantization effects in low power, low resolution ADPLLs. This, of course, presents a challenge in manual design of PLLs if simulation is an integral part to the most basic modeling, and thus motivates the creation of an automated design solution. Currently, no PLL design framework is known that automates PLL design for the needs of ultra low power PLLs as characterized here. Of the most prominent pre-existing frameworks, CppSim [\[add reference...\]](#) features a utility for design of continuous loop filters, however for this it does not provide any level of performance optimization, nor does it support discrete-time and quantized digital designs.

Thus in this paper, a new framework written in pure-Python is introduced, which uniquely addresses issues of ultra-low power ADPLL design. Specifically, design of integer-N type PLLs is focused on, as the impetus of this work is an integer-N PLL design project. Topics presented are (a) automatic design and optimization of ADPLL loop filters given target system and component level specs for the PLL, and (b) behavioral time domain PLL simulation for accurate analysis and verification of PLL performance, with an integrated Monte-Carlo sampling variation analysis engine.

A brief outline of the paper is as follows. An introduction to PLL theory is in section 2. [Simulation and optimization methods are discussed in section XX.](#) An example design exercise, a comparison to existing solutions, and general discussion considerations for using the framework are in section 6. Finally, section 7 concludes.

The main contributions of this work to PLL design are:

- Fully automatic PLL loop filter design and optimization of all digital PLLs from high level specifications in an open source framework.
- Integrated behavioral time domain simulation of integer-N digital PLLs for verification of filter and PLL design, with variational analysis of performance and stability.

2 Theory

In its most basic form, a phase locked loop is a phase-based feedback system whose output tracks or maintains a fixed phase relationship to an input signal. As will be shown, such a system is uniquely suited to the task of frequency synthesis, which is the process of generating derivative frequencies from some reference frequency. Given reference and output phase signals Φ_{ref} and Φ_{out} , a PLL can be modeled as in figure 1, with feedforward and feedback networks $A(s)$ and $B(s)$.

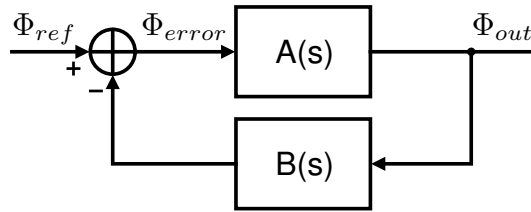


Figure 1: Basic phase feedback network.

The closed loop phase response $T(s)$ for Φ_{ref} to Φ_{out} is therefore:

$$T(s) = \frac{\Phi_{out}(s)}{\Phi_{ref}(s)} = \frac{A(s)}{1 + A(s)B(s)} \quad (1)$$

A particular case of interest is when $B(s) = 1/N$, where N is a constant, and the loop gain $A(s)B(s) \gg 1$, the closed loop response is:

$$\frac{\Phi_{out}(s)}{\Phi_{ref}(s)} \approx \frac{A(s)}{A(s)B(s)} = \frac{1}{B(s)} = N \quad (2)$$

We see that the phase through the PLL is multiplied by a factor of N . If the input phase signal is a sinusoid with frequency ω_{ref} , and likewise the output with ω_{out} , then $\phi_{ref}(t) = \omega_{ref}t$ and $\phi_{out}(t) = \omega_{out}t$. Thus:

$$\frac{\Phi_{out}(t)}{\Phi_{ref}(t)} = \frac{\omega_{out}t}{\omega_{ref}t} \approx N \quad \rightarrow \quad \omega_{out} \approx N\omega_{ref} \quad (3)$$

Therefore, it is observed that a PLL allows for the generation, i.e. synthesis, of a new frequency from a reference frequency signal. Given a feedback divider ration of $1/N$, the PLL multiplies the reference frequency by a factor of N . In the following sections, more advanced models for PLL will be developed, extending the concept introduced here. Specifically, the theory of digital, discrete-time PLLs will be developed and extended from a continuous phase model of a basic PLL.

2.1 Continuous PLL Model

Although PLLs are practically limited to using discrete-time sampling in real-world hardware, continuous models can still be applied in their analysis and design. Thus a continuous PLL model is developed in this section to aid in the later discussed discretized PLL modeling.

2.1.1 PLL Synthesizer architecture

The traditional architecture for implementing a PLL frequency synthesizer [5] is shown in figure 2. This basic PLL is comprised of four components: (1) a phase detector, denoted by PD, (2) a loop filter, denoted by $H_{LF}(s)$, (3) a voltage controlled oscillator, denoted by VCO, and (4) and phase divider, denoted by " $\div N$ " in the figure. These components are explained in the following sections.

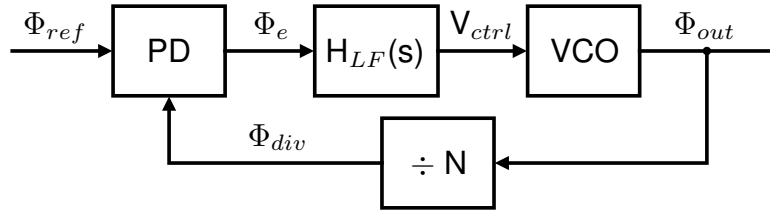


Figure 2: Basic PLL.

2.1.2 Divider

The phase divider is used as the feedback path in the PLL, where the division modulus N controls the frequency multiplication of the PLL. The transfer function of the divider is:

$$H_{div}(s) = \frac{\Phi_{div}(s)}{\Phi_{out}(s)} = \frac{1}{N} \quad (4)$$

2.1.3 Phase detector

The phase detector is used to measure the phase of the feedback signal (i.e. divider output) in relation to the reference phase, in order to establish a phase error signal Φ_e used to control the tuning of the PLL.

$$\Phi_e(s) = \Phi_{ref}(s) - \Phi_{div}(s) \quad (5)$$

2.1.4 Loop Filter

The PLL loop filter is used to control the phase-frequency response of PLL, which affects transient PLL behavior, as well as phase noise performance (see section 2.3). As will later be seen, low pass response is desired in a PLL, so the loop filter must be designed accordingly. Generally, this can be designed arbitrarily to have P poles and Z zeros, as such:

$$H_{LF}(s) = \frac{\sum_0^Z b_j s^j}{\sum_0^P a_k s^k} \quad (6)$$

Rational choice of the loop filter will ensure that the PLL will be stable and minimize steady state phase error. In order to achieve zero steady state error, the loop filter must contain a pole at zero, in other words an integrator. A PLL containing such a pole is classified as a Type II

PLL, and a PLL omitting the pole is considered Type I. A logical approach to loop filter design for zero-phase error is to treat it as a PID controller, where:

$$H_{LF}(s) = sK_d + K_p + \frac{K_i}{s} = \frac{K_d}{s} \left(s^2 + s\frac{K_p}{K_d} + \frac{K_i}{K_d} \right) \quad (7)$$

Such a loop filter contains two zeros and one integrator pole at zero. The gain parameters K_p, K_i, K_d can be tuned to achieve the desired bandwidth and stability for the PLL. The impacts of loop filter design will be further considered in sections 2.1.6-2.1.9.

2.1.5 VCO

The voltage controlled oscillator is an oscillator with frequency controlled by an input signal V_{ctrl} . The VCO is characterized by its gain $K_{DCO} = \partial f / \partial V_{ctrl}$, and the nominal oscillation frequency f_0 . Analyzed in terms of phase, an oscillator can be seen as a time-phase integrator:

$$\Phi_{VCO}(t) = \Phi_{out}(t) = \int 2\pi(K_{DCO}V_{ctrl}(t) + f_0)dt \quad (8)$$

In s-domain, where frequency offsets will be represented via initial conditions for modeling purposes, the VCO transfer function is therefore:

$$H_{VCO}(s) = \frac{\Phi_{VCO}(s)}{V_{ctrl}(s)} = \frac{\Phi_{out}(s)}{V_{ctrl}(s)} = \frac{2\pi K_{DCO}}{s} \quad (9)$$

2.1.6 Continuous PLL Transfer function

Now that the continuous PLL synthesizer is understood at a component level, the closed loop dynamics of the PLL can be analyzed. First the PLL loop gain is determined:

$$L(s) = H_{LF}(s)H_{VCO}(s)H_{div}(s) = \frac{2\pi K_{VCO}K_d}{N} \frac{1}{s^2} \left(s^2 + s\frac{K_p}{K_d} + \frac{K_i}{K_d} \right) \quad (10)$$

With the phase detector as the feedback summation point, the closed loop response of the PLL from reference to output is:

$$T(s) = \frac{\Phi_{out}(s)}{\Phi_{ref}(s)} = \frac{2\pi K_{VCO}(s^2 K_d + sK_p + K_i)}{s^2 \left(1 + \frac{2\pi K_{VCO}K_d}{N} \right) + \frac{2\pi K_{VCO}}{N}(sK_p + K_i)} = N \frac{L(s)}{1 + L(s)} \quad (11)$$

It should be noted that in the closed loop configuration, this PLL phase transfer function contains two poles and two zeros. This is not a low pass response as desired for a satisfactory PLL phase noise power spectrum, as will later be discussed. In order achieve low pass operation, the derivative term K_d must be set to zero, yielding a PI controller for the loop filter (with one zero and two poles):

$$T(s) = \frac{\Phi_{out}(s)}{\Phi_{ref}(s)} = \frac{2\pi K_{VCO}(sK_p + K_i)}{s^2 + \frac{2\pi K_{VCO}}{N}(sK_p + K_i)} = N \frac{L(s)}{1 + L(s)} \quad (12)$$

Steady state zero phase error can be verified by solving the closed loop $\Phi_e(s)$ for $s=0$:

$$\Phi_e(s)|_{s=0} = \left(\Phi_{ref}(0) - \frac{\Phi_{out}(0)}{N} \right) = \Phi_{ref}(0) \left(1 - \frac{\Phi_{out}(0)}{N\Phi_{ref}(0)} \right) = \Phi_{ref}(0) \left(1 - \frac{N}{N} \right) = 0 \quad (13)$$

2.1.7 PI-loop filter design

Given a PI-controller loop filter, which can be optionally represented using a pole at zero and a zero with $\omega_z = K_i/K_p$:

$$H_{LF}(s) = K_p + \frac{K_i}{s} = \frac{K_i}{s} \left(\frac{s}{\omega_z} + 1 \right) \quad (14)$$

Selection of (not-necessarily optimal) PI controller gains can be easily derived from overall PLL settling time requirements. Suppose that settling time t_s is defined such that the PLL settles within $\pm\delta$ of the final value for a step input. If the initial and final PLL output frequencies are f_i and Nf_{ref} , and settling with $\pm f_{tol}$ is desired, $\delta = f_{tol}/|f_i - Nf_{ref}|$. Settling time is therefore:

$$t_s = -\tau \ln(\delta) \quad (15)$$

Thus, to find settling time, a value for the PLL time constant τ must be derived. Rewriting equation 12 with substitutions $\omega_z = K_i/K_p$ and $K = 2\pi K_{VCO}K_i/N$:

$$\frac{\Phi_{out}(s)}{\Phi_{ref}(s)} = N \cdot \frac{s\frac{K}{\omega_z} + K}{s^2 + s\frac{K}{\omega_z} + K} \quad (16)$$

If the second order denominator can be redefined in terms of a natural frequency ω_n and damping ζ , such that:

$$s^2 + s\frac{K}{\omega_z} + K = s^2 + s2\zeta\omega_n + \omega_n^2 \quad (17)$$

It is then found that $\omega_n = \sqrt{K}$, and $\omega_z = \sqrt{K}/2\zeta$. The poles of equation 16 are then located at $s = \zeta\sqrt{K} \pm \sqrt{K}\sqrt{1 - \zeta^2}$. The settling time of the PLL will be determined by the real portion of dominant pole of equation 16, specifically $\tau = 1/|\min(\Re(\{s_{p1}, s_{p2}\}))|$. Based on the pole-zero plot of figure 3, it can be observed that the dominant pole location is maximized with $\zeta = 1$. The pole-zero loci orientations are based on increasing ζ values. According to Razavi [4], ζ is usually "chosen to be $> \sqrt{2}/2$ or even 1 to avoid excessive ringing."

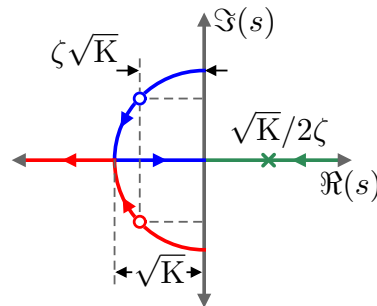


Figure 3: PI-controller PLL pole-zero locations.

To illustrate the effect of the damping coefficient ζ , figure 4 illustrates the example frequency and step responses of a PI-controlled PLL with $N=1$. Notice excessive peaking and ringing for $\zeta < \sqrt{2}/2$. The peaking observed in the frequency response is unavoidable with the PI-PLL due to the inherent zero in the transfer function. Its effect can be reduced with large ζ , however this will increase PLL settling time.

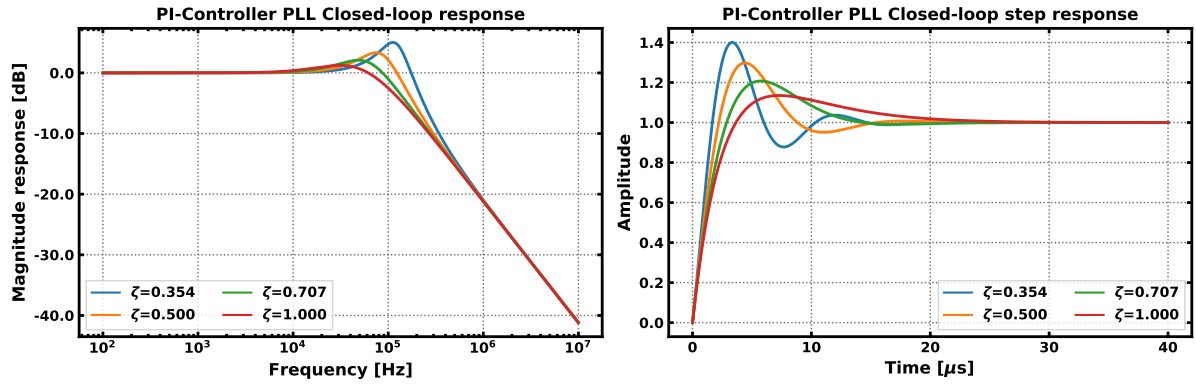


Figure 4: Example PI-PLL responses with varied ζ .

If ζ is constrained to ≤ 1 :

$$\tau = \frac{1}{|\min(\Re(\{s_{p1}, s_{p2}\}))|} = \frac{1}{\zeta\sqrt{K}} \quad (18)$$

Thus:

$$t_s = \frac{-\ln(\delta)}{\zeta\sqrt{K}} = \frac{-\ln\left(\frac{f_{tol}}{|f_i - Nf_{ref}|}\right)}{\zeta\sqrt{K}} \quad (19)$$

Based on specification for settling time and damping ζ , the values for K and ω_z can be determined. If K_{VCO} and N are also specified, the PI gain coefficients can be solved additionally.

$$\omega_z = \frac{-\ln(\delta)}{2t_s} = \frac{-\ln\left(\frac{f_{tol}}{|f_i - Nf_{ref}|}\right)}{2t_s} \quad (20)$$

$$K = \frac{\ln^2(\delta)}{\zeta^2 t_s^2} = \frac{\ln^2\left(\frac{f_{tol}}{|f_i - Nf_{ref}|}\right)}{\zeta^2 t_s^2} \quad (21)$$

$$K_i = \frac{NK}{2\pi K_{VCO}} \quad (22)$$

$$K_p = \frac{K_i}{\omega_z} \quad (23)$$

2.1.8 PI-controller peaking compensation

To compensate for closed loop peaking, the original PI-controller loop filter of equation 14 can be modified with the addition of a single tunable pole at ω_p . The closed loop response becomes third order, which complicates direct analysis and design of the loop filter. However, utilizing the automated filter optimization approach described later in this paper resolved issues regarding filter design in this case.

$$H_{LF}(s) = \frac{K_i \left(\frac{s}{\omega_z} + 1\right)}{s \left(\frac{s}{\omega_p} + 1\right)} \quad (24)$$

2.1.9 Alternative PID controller permutations

If individual terms within the PID-controller are dropped, different controller permutations (PD, ID, PI, P, I, D) can be achieved. As mentioned before, inclusion of an integral term is needed to ensure the desired zero steady state error for a PLL. This leaves ID and I-controllers as possible alternative solutions to PI for the loop filter. It is shown in the following that neither of these controllers result in a stable PLL, which leaves a PI-controller as the only viable PID implementation.

I-only controller

Setting the K_p and K_d terms of equation 11 to zero yields:

$$\frac{\Phi_{out}(s)}{\Phi_{ref}(s)} = \frac{2\pi K_{VCO} K_i}{s^2 + \frac{2\pi K_{VCO}}{N} K_i} \quad (25)$$

This closed loop transfer function results in a pair of poles at $\pm \sqrt{2\pi K_{VCO} K_i / N}$. This will never be stable, as it can only be manifested as (1) a pair of poles on the imaginary axis, which is an oscillator, or (2) a real pole in the right-half plane and a real pole in the left-half plane, the former of which is not causally stable.

ID-controller

Setting the K_p term of equation 11 to zero yields:

$$\frac{\Phi_{out}(s)}{\Phi_{ref}(s)} = \frac{2\pi K_{VCO} (s^2 K_d + K_i)}{s^2 \left(1 + \frac{2\pi K_{VCO} K_d}{N}\right) + \frac{2\pi K_{VCO}}{N} K_i} \quad (26)$$

The poles of this transfer have the same form as the I-only controller, and this PLL-controller configuration is unstable for the same reasons as the I-only controller PLL.

2.2 ADPLL - digital, discretized PLL Model

Based on the continuous PLL theory, a model for digital, discretized PLLs (i.e. ADPLLs) can be adapted. The general approach here is to utilize the bilinear transformation between continuous s-domain models to the discrete z-domain models. As commonly cited in PLL literature from a seminal paper by Gardner [2], if the sampling frequency $f_s > 10 \cdot BW_{loop}$, where BW_{loop} is the PLL loop bandwidth, the effects of time sampling are easily ignored for purposes of analysis. Thus the design methods established in this paper are predicated on $f_s > 10 \cdot BW_{loop}$.

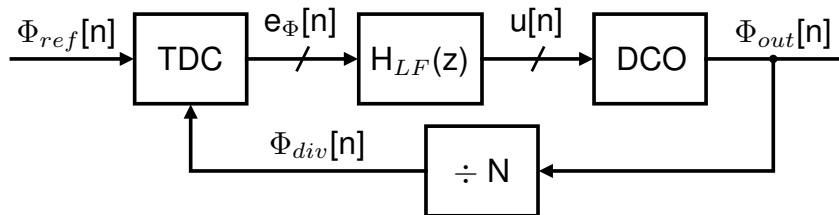


Figure 5: Basic ADPLL.

The basic architecture of an ADPLL is shown in figure 5. Here, compared to the continuous PLL, the phase detector has been replaced with a time to digital converter (TDC), the loop filter $H_{LF}(s)$ with a discrete loop filter $H_{LF}(z)$, and the VCO with a digitally controlled oscillator (DCO). In this architecture, the TDC, loop filter, and DCO are digital.

2.2.1 Divider

A digital divider functions by counting input cycles. With a divider modulus N , the output of the divider will have an active edge transition (considered to be rising edge as shown here) every N -cycles. Phase information is inferred from active edge timing, which occurs with time interval N/f_{osc} , and is equal to the point at which output phase equals a multiple of 2π . Thus a digital divider does not provide continuous phase information, but rather a sampled phase signal with rate f_{osc}/N .

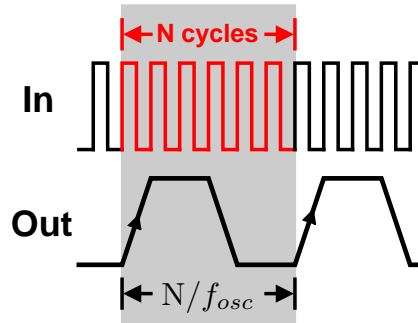


Figure 6: Digital divider signals.

For PLL transfer function modeling, a digital divider behaves identically to the continuous case:

$$\Phi_{div}[n] = \frac{\Phi_{out}[n]}{N} \quad (27)$$

Application of the z- and s-domain transformations:

$$H_{div}(z) = H_{div}(s) = \frac{\Phi_{div}(z)}{\Phi_{out}(z)} = \frac{1}{N} \quad (28)$$

2.2.2 TDC

The TDC is a digital, quantized representation of the the phase detector. It takes input phase signals $\Phi_{div}[n]$ and $\Phi_{ref}[n]$, and outputs a digital phase error word $e_\Phi[n]$. Figure 7 shows the basic TDC model architecture. Being digitized, a TDC will have limited resolution in phase, equivalent to M steps per reference cycle. This is a minimum step size in time of $\Delta t_{step} = 1/M f_{ref}$. Since the output of the TDC is digital, the model applies a scale factor $M/2\pi$ and floor rounding, so 1 least significant bit (LSB) of $e_\Phi[n]$ equates to Δt_{step} timing error between $\Phi_{div}[n]$ and $\Phi_{ref}[n]$.

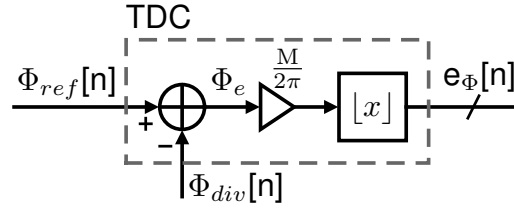


Figure 7: TDC model.

In sampled-time equation form:

$$e_{\Phi}[n] = \left\lfloor \frac{M}{2\pi} (\Phi_{ref}[n] - \Phi_{div}[n]) \right\rfloor \quad (29)$$

For purposes of PLL transfer function calculation, the TDC z- and s-domain representation is equation 31, which accounts for phase-to-digital domain conversion gain. Effects of quantization will be handled in section 2.3.

$$e_{\Phi}(z) = \frac{M}{2\pi} (\Phi_{ref}(z) - \Phi_{div}(z)) \quad (30)$$

$$H_{TDC}(z) = H_{TDC}(s) = \frac{M}{2\pi} \quad (31)$$

2.2.3 Loop Filter

The loop filter design will be derived from the continuous PI-controller loop filter with optional peaking compensation (equation 24) via application of the bilinear transform. The bilinear transform specifically allows for the conversion of a continuous transfer function to discrete representation, and vice versa. This, however is conditioned on satisfaction of Nyquist sampling criteria, and in the case of PLLs it is recommended that $f_s > 10 \cdot BW_{loop}$ to ensure transformation accuracy [2]. A high level of oversampling allows for the following definition of the bilinear transform, where $1/\Delta T_s = f_{ref}$:

$$\begin{aligned} z^{-1} &= e^{-s\Delta T_s} && \text{(definition of z-space)} \\ &= \sum_{k=0}^{\infty} \frac{(-s\Delta T_s)^k}{k!} && \text{(exponential Taylor series)} \\ &\approx 1 - s\Delta T_s && \text{(if } |s\Delta T_s| = 2\pi BW_{loop} \cdot \Delta T_s \ll 1) \end{aligned}$$

Thus the bilinear transform identities are:

$$z^{-1} = 1 - s\Delta T_s \quad (32)$$

$$s = \frac{1}{\Delta T_s} (1 - z^{-1}) \quad (33)$$

Applying 33 to equation 24 yields the z-domain loop filter:

$$H_{LF}(z) = H_{LF}(s) \Big|_{s=\frac{1}{\Delta T_s}(1-z^{-1})} = \frac{K_i \left(\frac{s}{\omega_z} + 1 \right)}{s \left(\frac{s}{\omega_p} + 1 \right)} \Big|_{s=\frac{1}{\Delta T_s}(1-z^{-1})} \quad (34)$$

$$= k_i \Delta T_s \frac{\omega_p}{\omega_z} \frac{(1 + \omega_z \Delta T_s) - z^{-1}}{(1 + \omega_p \Delta T_s) - z^{-1}(2 + \omega_p \Delta T_s) + z^{-2}} \quad (35)$$

Equation 35 is transformed to a digitally implementable representation by converting into the canonical representation of 36, which then determines the tap coefficients for the sampled-time difference equation 37.

$$H_{LF}(z) = \frac{\sum_{j=0}^M b_j z^{-j}}{1 + \sum_{k=1}^N a_k z^{-k}} \quad (36)$$

$$y[n] = - \sum_{k=1}^N a_k y[n-k] + \sum_{j=0}^M b_j x[n-j] \quad (37)$$

The transformed 35 is directly implementable in digital hardware with a direct type 1 IIR filter shown in figure 8, with the filter coefficients given by equations 38-41. The filter coefficients must be quantized into finite resolution fixed point words for a complete digital implementation. Effects of quantization will be discussed in section 2.3.

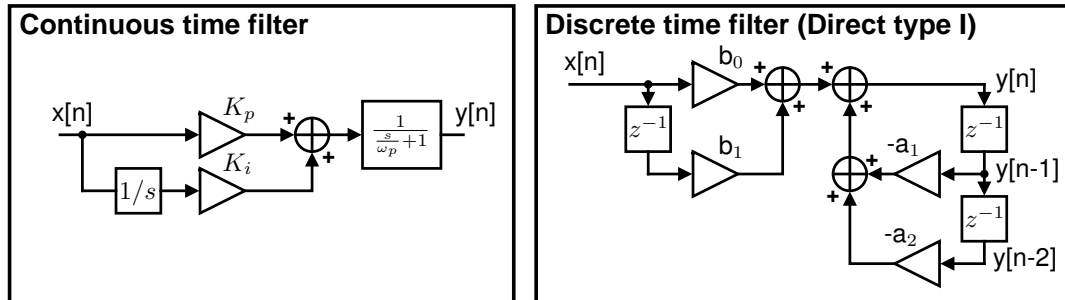


Figure 8: Implementation of filter.

$$a_1 = - \frac{2 + \omega_p \Delta T_s}{1 + \omega_p \Delta T_s} \quad (38)$$

$$a_2 = \frac{1}{1 + \omega_p \Delta T_s} \quad (39)$$

$$b_0 = \frac{K_i \omega_p \Delta T_s}{\omega_z} \frac{1 + \omega_z \Delta T_s}{1 + \omega_p \Delta T_s} \quad (40)$$

$$b_1 = \frac{K_i \omega_p \Delta T_s}{\omega_z} \frac{1}{1 + \omega_p \Delta T_s} \quad (41)$$

2.2.4 DCO

The digitally controlled oscillator varies from a VCO by only accepting a digital (quantized) frequency tuning signal, called the oscillator tuning word (OTW). A DCO modeled in discrete time as a recursive phase integrator, dependent on (a) the DCO gain K_{DCO} , equal to the

frequency tuning of the oscillator per OTW LSB , (b) the digital OTW $u[n]$, and (c) the sampling period $T = f_{ref}^{-1}$.

$$\Phi_{out}[n] = \Phi_{out}[n-1] + 2\pi K_{DCO} u[n] \Delta T_s \quad (42)$$

Application of the z-transform yields:

$$H_{DCO}(z) = \frac{\Phi_{out}(z)}{u(z)} = \frac{2\pi K_{DCO} \Delta T_s}{1 - z^{-1}} \quad (43)$$

Application of the bilinear transform to the DCO transfer function yields:

$$H_{DCO}(s) = \frac{\Phi_{out}(s)}{u(s)} = \frac{2\pi K_{DCO} \Delta T_s}{1 - (1 - s \Delta T_s)} = \frac{2\pi K_{DCO}}{s} \quad (44)$$

2.2.5 Discrete-time PLL transfer function

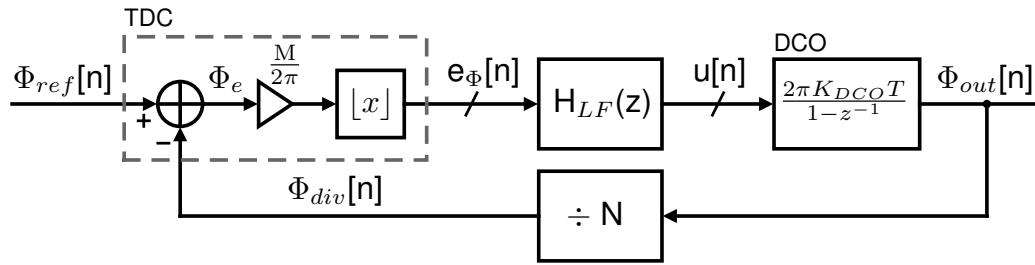


Figure 9: Discrete time PLL model.

The transfer function for the discrete-time PLL can be computed in the z-domain, and also approximated continuously. The open loop z-domain transfer function is:

$$L(z) = H_{TDC}(z)H_{LF}(z)H_{DCO}(z)H_{DIV}(z) \quad (45)$$

$$= 2\pi K_{DCO} K_i \Delta T_s^2 \frac{M}{N} \frac{\omega_p}{\omega_z} \frac{(1 + \omega_z \Delta T_s) - z^{-1}}{(1 + \omega_p \Delta T_s + 2\pi K_{DCO} K_i \Delta T_s^2 \frac{M}{N} \frac{\omega_p}{\omega_z} (1 + \omega_z \Delta T_s)) - z^{-1} (3 + 2\omega_p \Delta T_s) + z^{-2} (3 + \omega_p \Delta T_s) - z^{-3}} \quad (46)$$

The closed loop z-domain PLL phase transfer function is:

$$T(z) = \frac{\Phi_{out}(z)}{\Phi_{ref}(z)} = \frac{2\pi K_{DCO} K_i \Delta T_s^2 \frac{M}{N} \frac{\omega_p}{\omega_z} (1 + \omega_z \Delta T_s) - z^{-1}}{\left((1 + \omega_p \Delta T_s + 2\pi K_{DCO} K_i \Delta T_s^2 \frac{M}{N} \frac{\omega_p}{\omega_z} (1 + \omega_z \Delta T_s)) - z^{-1} (3 + 2\omega_p \Delta T_s) + z^{-2} (3 + \omega_p \Delta T_s) - z^{-3} \right)} \quad (47)$$

The s-domain approximation of the transfer function is:

$$L(s) = H_{TDC}(s)H_{LF}(s)H_{DCO}(s)H_{DIV}(s) = \frac{M}{N} \frac{K_{DCO} K_i}{s^2} \frac{\left(\frac{s}{\omega_z} + 1 \right)}{\left(\frac{s}{\omega_p} + 1 \right)} \quad (48)$$

And in closed loop configuration the s-domain PLL phase transfer function is:

$$T(s) = \frac{\Phi_{out}(s)}{\Phi_{ref}(s)} = \frac{MK_{DCO} K_i \left(\frac{s}{\omega_z} + 1 \right)}{s^3 \frac{1}{\omega_z} + s^2 + \frac{M}{N} K_{DCO} K_i \left(\frac{s}{\omega_z} + 1 \right)} = N \frac{L(s)}{1 + L(s)} \quad (49)$$

Incidentally, the s-domain approximation is significantly simpler and will be preferred in this paper for purposes of analysis.

2.3 ADPLL Noise Model

The noise in the discrete-time ADPLL results from quantization and from stochastic sources. Quantization results from round off errors introduced in the digitization of PLL components (in the TDC, loop filter, and DCO). Stochastic noise results from thermal and flicker noise in the PLL components when considered in an analog viewpoint (present in the DCO, divider and TDC). The noise generated by these quantization sources will be discussed in the following sections, based on a modeling and noise analysis approach from [3].

2.3.1 TDC noise

The predominant phase noise source in the TDC is due to quantization. A straightforward approach to model quantization noise is to utilize the model of figure 10b to represent quantization.

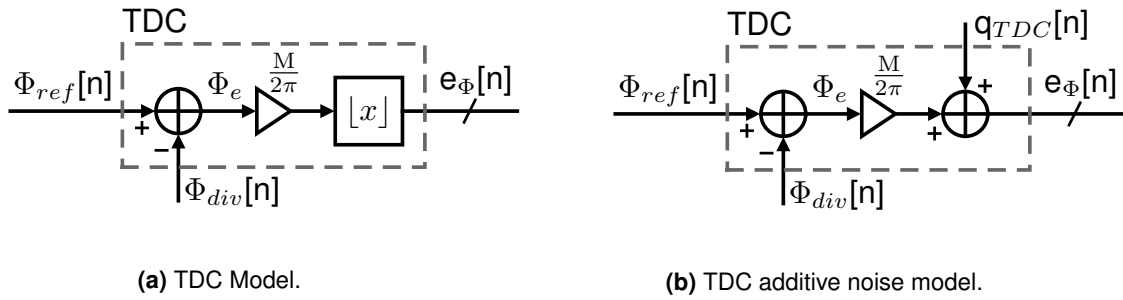


Figure 10: TDC quantization noise models.

Using this model, the quantized signal $e_\Phi[n]$ is the sum of its unquantized representation $\Phi_e \frac{M}{2\pi}$ with a quantization error signal $q_{TDC}[n]$. Figure 11 illustrates this process.

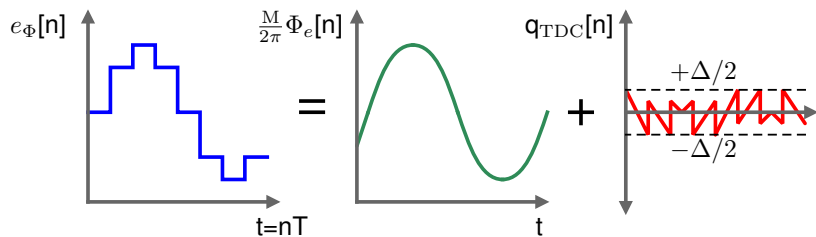


Figure 11: Quantization as via additive error signal.

The quantization noise signal has the statistical property that it is uniformly distributed in the range $[-\Delta/2, \Delta/2]$, i.e. $P_q(Q = q) = U(-\Delta/2, \Delta/2)$ if Δ is the quantization step size. The power of the TDC quantization noise signal is:

$$\sigma_{q_{TDC}}^2 = \int_{-\infty}^{\infty} q^2 P_q(Q = q) dq = \int_{-\Delta/2}^{\Delta/2} \frac{q^2}{\Delta} dq = \frac{\Delta^2}{12} \quad (50)$$

Since $e_\Phi[n]$ is digital signal, the minimum step size is $\Delta=1$ LSB. The TDC quantization noise power is therefore $\sigma_{qTDC}^2 = 1/12 \text{ LSB}^2$. The po If the quantization noise is assumed to be white, and the TDC is sampled at f_{ref} , the quantization PSD is:

$$S_{qnTDC}(f) = \frac{P_{qTDC}}{\Delta f} = \frac{\sigma_{qTDC}^2}{f_{ref}} = \frac{\Delta^2}{12f_{ref}} = \frac{1}{12f_{ref}} \frac{[\text{LSB}]^2}{[\text{Hz}]} \quad (51)$$

2.3.2 DCO noise

Add connection of DCO noise to random phase walk, cite Leeson Spectral dispresion from random phase walk [7].

Noise in a DCO is resulting from (a) quantization of the oscillator tuning word $u[n]$, and (b) from thermal and stochastic sources. In the digital PLL, the OTW quantization occurs in the loop filter, so this will be analyzed in the later loop filter section (2.3.4). Thus oscillator thermal/stochastic noise will be considered, to develop a phase noise model where oscillator phase noise Φ_{nDCO} is an additive process to the oscillator phase Φ_{osc} , thus $\Phi_{out} = \Phi_{osc} + \Phi_{nDCO}$.

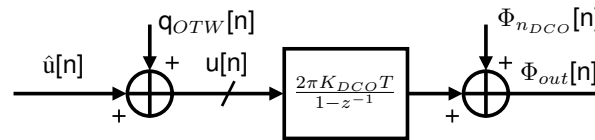


Figure 12: DCO additive noise model.

Oscillator phase noise due to stochastic and uncorrelated circuit and supply noise can be analyzed as additive voltage disturbance δv_n with variance $\sigma_{v_n}^2$ to the oscillator waveform V_{osc} at any given time. In a stable, noiseless oscillator, amplitude is inherently tied to signal phase, i.e. $V_{osc}(\Phi = \omega t)$. With additive noise, given $\frac{dV_{osc}(\Phi)}{d\Phi}$ is finite $\forall t$, a small voltage disturbance from noise δv_n will be coupled as a disturbance $\delta\Phi_n$ in the oscillator phase, shown in figure 13. The phase evolution of the noisy oscillator for an infinitesimal time increment δt with such a disturbance is:

$$\Phi_{out}(t + \delta t) = \Phi_{out}(t) + \delta\Phi_n + \omega_{osc}\delta t \quad (52)$$

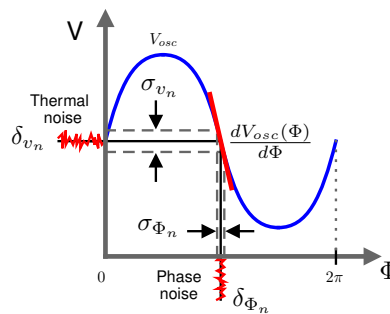


Figure 13: Voltage to phase noise conversion.

Assuming δv_n is Gaussian white noise, $\delta\Phi_n$ is sampled stochastically at any instant based on the probability distribution 53, dependent on the current oscillator phase Φ_{out} and the noiseless

voltage-phase relation $V_{osc}(\Phi)$. It will be assumed that like the source noise δv_n , $\delta\Phi_n$ is white spectrum.

$$P(\delta\Phi_n|\Phi_{out}) = \text{Norm} \left(\mu = 0, \sigma = \sigma_{v_n} \left(\frac{dV_{osc}(\Phi)}{d\Phi} \bigg|_{\Phi=\Phi_{out}} \right)^{-1} \right) \quad (53)$$

Spectral analysis of the noisy oscillator phase can be made utilizing discrete time-modeling. Converting 52 into a sampled signal with time step δt

$$\Phi_{out}[n+1] = \Phi_{out}[n] + \omega_{osc}\delta t + \delta\Phi_n[n|\Phi_{out}[n]] \quad (54)$$

Computing the z-transform, and splitting the result into the oscillation Φ_{osc} and phase noise Φ_n components:

$$\Phi_{out}(z) = \frac{\omega_{osc}\delta t}{z-1} + \frac{\delta\Phi_n(z)}{z-1} = \Phi_{osc}(z) + \Phi_n(z) \quad (55)$$

$$\Rightarrow \Phi_n(z) = \frac{\delta\Phi_n(z)}{z-1} \quad (56)$$

Application of the bilinear transform to 56 can be used to approximate the continuous phase noise spectrum, if $s = j\omega$

$$\Phi_n(s) = \Phi_n(z)|_{z=1-s\delta t} = \frac{\delta\Phi_n(z)}{z-1} \bigg|_{z=1+s\delta t} = \frac{\delta\Phi_n(s)}{s\delta t} \quad (57)$$

The phase noise PSD is therefore:

$$S_{\Phi_{nDCO}}(f) = \lim_{\Delta T \rightarrow \infty} \frac{1}{\Delta T} \left| \frac{\delta\Phi_n(j2\pi f)}{j2\pi f\delta t} * \mathcal{F} \left\{ \text{rect} \left(\frac{t}{\Delta t} \right) \right\} \right|^2 = \frac{S_{0\Phi_{nDCO}}}{f^2} \quad (58)$$

Following that the phase disturbance signal $\delta\Phi_n(t)$ is white spectrum, a constant value for its PSD $S_{0\Phi_{nDCO}}$ can be defined. The value for $S_{0\Phi_{nDCO}}$ is highly dependent on implementation and is best extracted by means of curve fitting simulation or physical measurement.

2.3.3 Divider noise

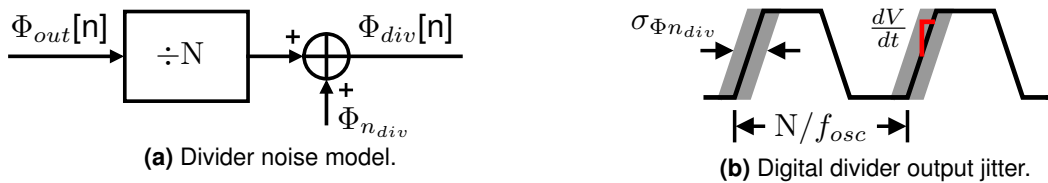


Figure 14: Divider phase noise.

Divider noise is manifested as jitter (with RMS distribution in time of $\sigma_{tn_{div}}$) on the the divider output. This is due to effects of stochastic and uncorrelated voltage noise coupling into the signal phase, much like in the case of oscillator phase noise. If the divider is a digital circuit, with edge rate dV/dt , and subject to thermal noise in the form of a voltage v_n , with noise power of $\sigma_{v_n}^2$, the divider phase noise power added to the divider output is:

$$\sigma_{\Phi_{n_{div}}}^2 = \omega_{ref}^2 \sigma_{tn_{div}}^2 = \omega_{ref}^2 \left(\frac{dV}{dt} \right)^{-2} \sigma_{v_n}^2 \quad (59)$$

At lock, the output of a digital divider will have an update rate $f_{osc}/N \approx f_{ref}$, which can be treated as the sampling rate of the output phase signal $\Phi_{div}[n]$. Thus if the divider phase noise power is confined into a bandwidth equal to f_{ref} , the spectral density of divider noise is:

$$S_{\Phi_{div}}(f) = \frac{\sigma_{\Phi_{div}}^2}{f_{ref}} = 2\pi\omega_{ref}\sigma_{v_n}^2 = 2\pi\omega_{ref} \left(\frac{dV}{dt} \right)^{-2} \sigma_{v_n}^2 \frac{[\text{rad}]^2}{[\text{Hz}]} \quad (60)$$

2.3.4 Loop filter noise - direct type I

In a digital loop filter, quantization noise arises from rounding errors due to finite precision in the arithmetic circuits that implement the filter. Quantization noise power here will be derived under the assumption of a direct type-I filter implementation, with B bits in each fixed point word throughout the loop filter. In a digital implementation of the canonical z-domain transfer function 61 as the direct type-I structure of figure 15a, delays are constructed using registers, adders with digital adders, and the filter coefficient gain terms $\{a_1, \dots, a_N; b_0, \dots, b_M\}$ with digital multipliers. The registers and adders do not introduce extra round-off error beyond that already existing, however the multipliers will if the products of B bit words, yielding 2B bits, are mapped onto B bit words.

$$H_{LF}(z) = \frac{\sum_{j=0}^Z b_j z^{-j}}{1 + \sum_{k=1}^P a_k z^{-k}} \quad (61)$$

Quantization in this case can be represented by adding a quantization error signal $q_x[n]$ to the result of each ideal multiplication, as shown in figure 15b. This is the same approach for TDC quantization noise in section 50. The noise power associated with each $q_x[n]$ is identical, with $\sigma_{qx}^2 = 1/12 \text{ LSB}^2$.

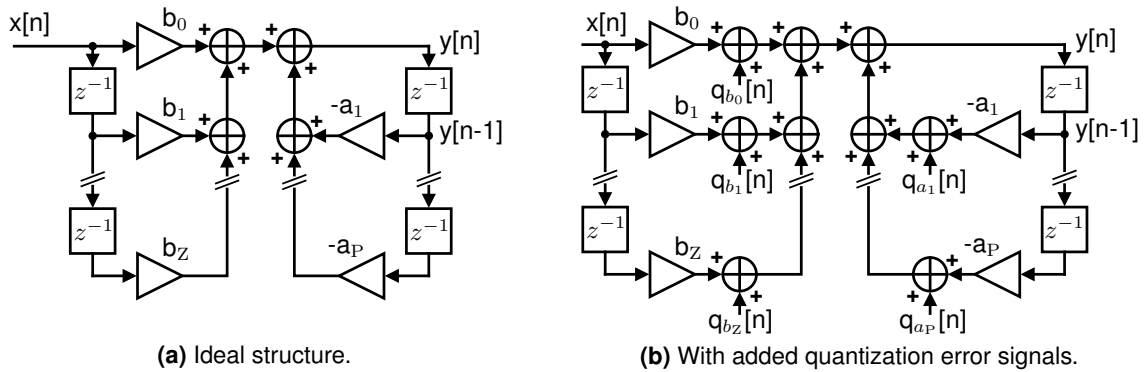


Figure 15: Direct type I filter implementation with quantization.

Assuming the quantization error signals of each multiplier are uncorrelated with all other multipliers, the output-referred noise power of the filter can be computed as the sum of the output-referred individual contributions. These contributions can be determined via solving for the transfer function from each source $q_x[n]$ of each quantization noise to the output $y[n]$. In the case of the direct type I filter structure, all quantization sources $q_x[n]$ have the same transfer characteristic to the output $y[n]$:

$$\frac{Y(z)}{Q_x(z)} = \frac{1}{1 + \sum_{k=1}^P a_k z^{-k}} \quad (62)$$

Applying the bilinear transform to 62, with high oversampling where $N \cdot BW_{loop} 10 < f_{ref}$, and N is the number of poles in the system.

$$\left. \frac{Y(z)}{Q_x(z)} \right|_{z^{-1}=1-sT} \approx \frac{1}{1 + \sum_{k=1}^P a_k - s \sum_{k=1}^P k a_k} \quad (63)$$

The output power spectral density is then for one error source is, confined to a bandwidth defined by the (sampling) reference frequency f_{ref} :

$$S_{qx}(f) = \frac{\sigma_{qx}^2}{f_{ref}} \left| \frac{Y(s)}{Q_x(s)} \right|_{s=j2\pi f}^2 \approx \frac{1}{12f_{ref}} \left| \frac{1}{1 + \sum_{k=1}^P a_k - j2\pi f \sum_{k=1}^P k a_k} \right|^2 \frac{[\text{LSB}]^2}{[\text{Hz}]} \quad (64)$$

Given P poles and Z zeros in the filter, the total output quantization PSD of the filter is 65. The total loop filter noise PSD linearly scales with the number of multipliers in the direct type-I filter implementation.

$$S_{qn_{LF}}(f) = (P + Z + 1) S_{qx}(f) \frac{[\text{LSB}]^2}{[\text{Hz}]} \quad (65)$$

2.3.5 PLL noise sensitivity transfer functions

Having developed models for noise of generated by each PLL component, noise sensitivity transfer functions must be computer to refer each noise source to the PLL output in terms of phase. In the developed noise theory, thus far all noise sources have been modeled as additive phase components. The full system model illustrating this is:

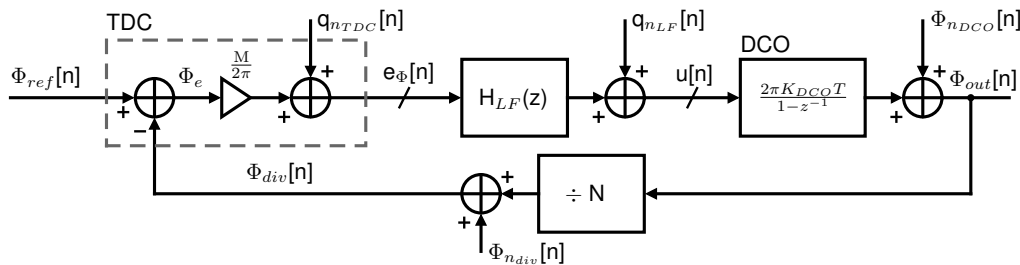


Figure 16: Full PLL additive noise model.

It is useful to define a transfer function $\hat{T}(s)$ which characterizes the normalized closed loop response from reference to output of the PLL. $\hat{T}(s)$ is defined in terms of the loop gain $L(s)$.

$$\hat{T}(s) = \frac{L(s)}{1 + L(s)} \quad \text{s.t.} \quad T(s) = \frac{\Phi_{out}}{\Phi_{ref}} = N\hat{T}(s) \quad (66)$$

Solving for the closed transfer functions between each q_{nTDC} , q_{nLF} , Φ_{nDCO} and Φ_{ndiv} to the

output Φ_{out} utilizing s-domain approximations yield:

$$\frac{\Phi_{out}(s)}{q_{n_{TDC}}(s)} = \frac{2\pi \frac{K_{DCO}}{s} H_{LF}(s)}{1 + L(s)} = 2\pi \frac{N}{M} \frac{L(s)}{1 + L(s)} = 2\pi \frac{N}{M} \hat{T}(s) \quad (67)$$

$$\frac{\Phi_{out}(s)}{\Phi_{n_{DCO}}(s)} = \frac{1}{1 + L(s)} = 1 - \hat{T}(s) \quad (68)$$

$$\frac{\Phi_{out}(s)}{q_{n_{LF}}(s)} = \frac{2\pi \frac{K_{DCO}}{s}}{1 + L(s)} = 2\pi \frac{K_{DCO}}{s} (1 - \hat{T}(s)) \quad (69)$$

$$\frac{\Phi_{out}(s)}{\Phi_{n_{div}}(s)} = \frac{M \frac{K_{DCO}}{s} H_{LF}(s)}{1 + L(s)} = N \frac{L(s)}{1 + L(s)} = N \hat{T}(s) \quad (70)$$

2.3.6 PLL phase noise and output PSD relationship

When analyzing PLL noise, the noise power spectral density of the PLL output is of most interest. Up to this point, noise has been defined in terms of phase noise Φ_n , or an unwanted added component to the oscillator phase signal $\Phi_{osc} = \omega_{osc}t$. The PLL output phase signal Φ_{out} is thus:

$$\Phi_{out}(t) = \Phi_{osc}(t) + \Phi_n(t) = \omega_{osc}t + \Phi_n(t) \quad (71)$$

Computation of PSD requires the PLL output voltage waveforms. These here will be defined in terms of complex exponentials. Given an oscillation amplitude A_0 :

$$V_{out} = \Re(A_0 e^{j\Phi_{out}(t)}) = \Re(A_0 e^{j\omega_{osc}t} e^{j\Phi_n(t)}) \quad (72)$$

Assuming the phase noise signal is zero mean, $\mathbb{E}[\Phi_n(t)] = 0$, and the power of phase noise signal is small, $\text{Var}[\Phi_n(t)] \ll 1$, then the approximation $e^{j\Phi_n(t)} = 1 + j\Phi_n(t)$ can be applied by truncating the exponential Taylor series expansion.

$$V_{out} = \Re(A_0 e^{j\omega_{osc}t} e^{j\Phi_n(t)}) = \Re(A_0 e^{j\omega_{osc}t} + j\Phi_n(t) A_0 e^{j\omega_{osc}t}) \quad (73)$$

$$= A_0 \cos(\omega_{osc}t) - \Phi_n(t) A_0 \sin(\omega_{osc}t) \quad (74)$$

The result is a carrier cosine signal, and an orthogonal sine signal modulated by the phase noise Φ_n . From this, the spectral density of the phase noise relative to the carrier can be estimated. The power spectral density $S_{V_{out}}$ is computed in 75-77. Due to orthogonality of the sine/cosine components of 74, the cross terms that appear in the PSD are zero.

$$S_{V_{out}} = \lim_{\Delta T \rightarrow \infty} \frac{1}{\Delta T} |\mathcal{F}\{V_{out}(t) \cdot \text{rect}(t/\Delta T)\}|^2 \quad (75)$$

$$= \lim_{\Delta T \rightarrow \infty} \frac{A_0^2}{\Delta T} |\mathcal{F}\{\cos(\omega_{osc}t) \cdot \text{rect}(t/\Delta T)\}|^2 \quad (76)$$

$$+ \lim_{\Delta T \rightarrow \infty} \frac{A_0^2}{\Delta T} |\mathcal{F}\{\Phi_n(t) \cdot \text{rect}(t/\Delta T)\} * \mathcal{F}\{\sin(\omega_{osc}t) \cdot \text{rect}(t/\Delta T)\}|^2 \quad (77)$$

Single side band (SSB) noise power spectral density $\mathcal{L}(\Delta f)$ is defined as the phase noise PSD at offset Δf from the carrier frequency f_{osc} , normalized to the carrier power. Here the PSD carrier component is given by 76, and the noise component by 77.

$$\mathcal{L}(\Delta f) = \lim_{\Delta T \rightarrow \infty} \frac{1}{\Delta T} |\mathcal{F}\{\Phi_n(t) \cdot \text{rect}(t/\Delta T)\}|^2 \Big|_{f=\Delta f} = S_{\Phi_n}(\Delta f) \quad (78)$$

Thus, the PLL output noise PSD relative to the carrier is equal to the PSD $S_{\Phi_n}(\Delta f)$ of the phase noise signal $\Phi_n(t)$.

2.3.7 PLL output-referred noise PSD

In terms of analysis, PLL noise PSD referred to the PLL output is of most interest. Thus far the following have been established: (a) noise spectrum generated by each individual PLL component, (b) the PLL phase noise sensitivity functions, and (c) the relationship between PLL output PSD and output phase noise. Now these can be combined to provide a final result for full PLL output-referred noise PSD. An important assumption here is all noise sources are uncorrelated, so their independent noise power contributions may be summed to find the total noise PSD. The PLL output phase noise PSD for each noise source is simply found by multiplying magnitude squared of the respective noise sensitivity function with the noise source PSD. Thus:

$$S_{\Phi_{n_{TDC},out}}(f) = S_{q_{n_{TDC}}}(f) \left| \frac{\Phi_{out}(f)}{q_{n_{TDC}}(f)} \right|^2 = \frac{1}{12f_{ref}} \left| 2\pi \frac{N}{M} \hat{T}(f) \right|^2 \quad (79)$$

$$S_{\Phi_{n_{DCO},out}}(f) = S_{\Phi_{n_{DCO}}}(f) \left| \frac{\Phi_{out}(f)}{\Phi_{n_{DCO}}(f)} \right|^2 = \frac{S_{0\Phi_{n_{DCO}}}}{f^2} \left| 1 - \hat{T}(f) \right|^2 \quad (80)$$

$$S_{\Phi_{n_{LF},out}}(f) = S_{q_{n_{LF}}}(f) \left| \frac{\Phi_{out}(f)}{q_{n_{LF}}(f)} \right|^2 \approx \frac{K_{DCO}^2}{12f_{ref}f^2} \left| \frac{1 - \hat{T}(f)}{1 + \sum_{k=1}^P a_k - j2\pi f \sum_{k=1}^P k a_k} \right|^2 \quad (81)$$

$$S_{\Phi_{n_{div},out}}(f) = S_{\Phi_{n_{div}}}(f) \left| \frac{\Phi_{out}(f)}{\Phi_{n_{div}}(f)} \right|^2 = f_{ref} \left| 2\pi \sigma_{tn_{div}} N \hat{T}(f) \right|^2 \quad (82)$$

The output SSB noise PSD at offset Δf relative to the carrier normalized to carrier power of PLL will be:

$$\mathcal{L}(\Delta f) = S_{\Phi_{n_{TDC},out}}(\Delta f) + S_{\Phi_{n_{DCO},out}}(\Delta f) + S_{\Phi_{n_{LF},out}}(\Delta f) + S_{\Phi_{n_{div},out}}(\Delta f) \quad (83)$$

Hypothetical ex. plot of all components? (in disco?)

3 ADPLL Design Automation

Design automation for ADPLL loop filter is implemented with a strategy that utilizes a continuous time-approximation based model of the PLL to generate a pseudo-optimum loop filter design, and then performs discrete time conversion and digitization of the design. Second order optimization is then applied to the discretized and digitized filter implementation, to minimize effects of quantization error and filter design error due to finite word effects. A discrete-time, behavioral PLL simulator is then used to verify the filter design for proper lock-time, phase noise and stability.

The design automation approach utilizes a fixed form of a loop filter as a prototype for all loop filter designs.

3.1 Loop filter

3.2 Design sequence

4 Behavioral ADPLL simulation

To fully capture the effects of a discrete time PLL with digital quantization effects, the implementation a behavioral, discrete event PLL simulator is described in the following. The simulator utilizes behavioral models to describe the individual components which comprise the PLL. These components are (1) a clock reference, (2) a TDC, (3) a loop filter, (4) a DCO, and (5) a divider. These behavioral models fully encapsulate effects of time-quantization and digitization. The simulator operates by iterating in fixed time steps of $\Delta t = 1/f_s$, where each node in the PLL is updated based upon the previous node values in a manner that is defined by each PLL component behavioral model. Each behavioral model is represented programmatically utilizing classes. In simulation, each component instance is represented by a object instance of the respective model class, constructed with any initial parameters (such as division ratio) that describe the component.

Define simulation parameters

Configuration parameters

Reference frequency <code>fref</code>	DCO gain <code>kdco</code>	Initial frequency error <code>init_f_error</code>
Divider modulus <code>div_n</code>	DCO nominal frequency <code>dco_f0</code>	Loop filter <code>lf_params</code>
TDC resolution <code>tdc_steps</code>	DCO phase noise power <code>dco_pn</code>	Simulation steps <code>sim_steps</code>

Initialize simulation

Instantiate model class objects

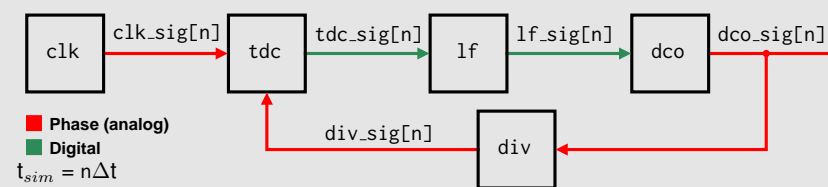
<code>clk</code>	<code>lf</code>	<code>div</code>
<code>tdc</code>	<code>dco</code>	

Initialize simulation data arrays

<code>clk_sig[n]</code>	<code>lf_sig[n]</code>	<code>div_sig[n]</code>
<code>tdc_sig[n]</code>	<code>dco_sig[n]</code>	

Run simulation

for n in range(simulation_steps):



Post-processing

Extract data and plot results

Phase noise spectrum	Transient responses
Lock time	

Figure 17: Simulation process.

The discrete event simulator is given in the following pseudocode, with component model objects `{clk, tdc, lf, dco, div}`, and simulation data arrays `{clk_sig, tdc_sig, lf_sig, dco_sig, div_sig}`. Each model object is updated at each simulation step utilizing the class method `update`, passing any relevant simulation data as arguments to the method.

```

1 for n in range(simulation_steps):
2     clk_sig[n] = clk.update()
3     tdc_sig[n] = tdc.update(clk_sig[n-1], div_sig[n-1])
4     lf_sig[n] = lf.update(tdc_sig[n-1], clk_sig[n-1]) #loop filter

```

```

5     osc_sig[n] = dco.update(lf_sig[n-1])
6     div_sig[n] = div.update(osc_sig[n-1], div_n)

```

Listing 1: PLL simulation loop Python pseudocode

After the simulation loop reaches completion, the results stored in the simulation data arrays can be post-processed to extract phase noise data, transient behavior and lock time. The following sections will discuss in more detail the implemented behavioral model classes and post-processing.

4.1 Clock behavioral model

An ideal behavioral clock model is utilized. The model is instantiated with the clock frequency f and the simulator time step dt . The model incrementing its phase every simulation step by a fixed amount $\Delta\Phi = 2\pi f \cdot dt$. The model outputs an analog phase signal.

```

1 class Clock:
2     def __init__(self, f, dt):
3         self.f = f          # clock frequency
4         self.dt = dt        # simulation time step
5         self.phase = 0.0    # clock phase state variable
6
7     def update(self):
8         self.phase += 2*pi*self.f*self.dt    # increment phase
9         return self.phase

```

Listing 2: Ideal clock behavioral model.

4.2 TDC behavioral model

The TDC behavioral model takes two analog inputs x and y that are in units of phase, and outputs a digital word that quantifies the phase separation of the signals. The model is instantiated with a resolution parameter tdc_steps , which defines the number of phase steps per cycle of the reference input x the TDC can resolve. The method `round` quantizes an floating point argument to the nearest integer.

```

1 class TDC:
2     def __init__(self, tdc_steps):
3         self.tdc_steps = tdc_steps
4
5     def update(x, y):
6         ph_error = wrap(x-y)    # wraps phase to be within [0, 2*pi]
7         return round(self.tdc_steps*(ph_error/(2*pi)))

```

Listing 3: TDC behavioral model.

4.3 Loop filter behavioral model

The loop filter model implements a discrete-time filter via difference equation that operates on input x . The equivalent of one pole and two zeros are modelled, described using the filter

coefficients $\{a_1, a_2; b_0, b_1\}$:

$$H_{LF}(z) = \frac{b_0 + b_1 z^{-1}}{a_0 + a_1 z^{-1} + a_2 z^{-2}} \quad (84)$$

$$y[n] = -a_1 y[n-1] - a_2 y[n-2] + b_0 x[n] + b_1 x[n-1] \quad (85)$$

Pseudocode for implementation of the model class is as follows. Data is to be represented with fixed point format, with number of fractional bits `frac_bits` and number of integer bits `int_bits`. The method `fixed_point` rounds floating point values to be equivalent to the nearest representation in the desired fixed point format. The filter coefficients are assumed to be pre-converted to the desired fixed-point equivalent values, and input `x` is assumed to be integer-valued.

```

1 class LoopFilter:
2     def __init__(self, a1, a2, b0, b1, int_bits, frac_bits):
3         self.a1 = a1; self.a2 = a2
4         self.b0 = b0; self.b1 = b1
5         self.xprev1 = 0;
6         self.yprev1 = 0; self.yprev2 = 0
7         self.int_bits=int_bits; self.frac_bits=frac_bits
8
9     def update(x):
10        ynew = -self.a1*self.yprev1 - self.a2*self.yprev2 \
11              + self.b0*x + self.b1*self.xprev1 # difference equation
12        self.yprev2 = self.yprev1
13        self.yprev1 = fixed_point(ynew, self.int_bits, self.frac_bits)
14        self.xprev1 = x
15        return round(self.yprev1) # convert to integer

```

Listing 4: Loop filter behavioral model.

4.4 DCO behavioral model

The DCO is modeled similar to the clock model, with the inclusion of a digital input `otw` for tuning the frequency. Nominal oscillator frequency is given by `f0`, and the DCO gain in Hz/LSB of `otw` is `kdco`. Additionally, oscillator phase noise modeling is included utilizing additive random phase walk (see section 2.3.2). Random walk is implemented by stochastically adding or subtracting a fixed magnitude random walk phase increment `krw` to the oscillator phase every simulation step. The sign of `krw` is randomly chosen with equal probability for positive and negative, implemented with the method `choice`.

```

1 class DCO:
2     def __init__(self, f0, kdco, krw):
3         self.f0 = f0 # nominal frequency
4         self.kdco = kdco # DCO gain
5         self.krw # random phase walk gain
6         self.phase = 0 # phase state variable
7
8     def update(otw):
9         self.phase += 2*pi*(f0 + otw*kdco) + krw*choice([-1,1])
10        return self.phase

```

Listing 5: DCO behavioral model.

4.5 Divider behavioral model

The divider model is defined with the divider modulus `div_n` and only performs a simple division of input phase.

```
1 class Divider:
2     def update(x, div_n):
3         return x/div_n
```

Listing 6: Divider behavioral model.

4.6 Post processing: lock time detection

Lock time detection of the PLL start-up transient can be determined from the simulation data conditioned on a tolerance band for acceptable frequency error `lock_f_tol` is provided to the simulator by the user. Since the desired frequency of the PLL $f_{osc} = \text{div_n} \cdot f_{ref}$, nominal oscillator frequency `dco_f0` and simulation conditions of the PLL are known by the simulator, the ideal value of the loop filter at lock, `lf_lock_ideal` can be computed directly. Given the DCO gain value in the simulation `kdco`, the value of `lf_lock_ideal = round((fosc - dco_f0)/kdco)`. Lock is then detected at the first simulation step for which the current and all later time steps meet the following criteria for the loop filter signal `lf_sig` (i.e. frequency of oscillator is within the frequency tolerance band):

$$\text{abs}(\text{lf_sig}[n] - \text{lf_lock_ideal}) \cdot \text{kdco} < \text{lock_f_tol} \quad (86)$$

This measurement is predicated on the simulation being fully complete at the time of measurement. Lock time is computed by multiplying the simulation index of lock with the simulation time step, $1/f_s$.

4.7 Post processing: phase noise power spectrum estimate

The simulation data can be used to make an estimate of the single side band phase noise power spectrum $\mathcal{L}(\Delta f)$ of the PLL (normalized to the carrier power). First, the phase error signal of the simulated PLL must be computed, `phase_error = div_n*clk_sig - osc_sig`. The phase error signal includes the phase noise signal in addition to any transient phase error components of the PLL. If the simulated PLL is in lock, the phase error can be dominated by phase noise components, as the transient components become negligible. If `phase_error` is reduced to the simulation signal span after the detection of lock, with a span in samples of `n_steps`, the power spectral density of the phase noise normalized to the carrier tone, utilizing the fast Fourier transform (FFT) is:

$$\text{psd} = \left| \frac{1}{n_steps} \cdot \mathcal{FFT}\{\text{div_n} \cdot \text{clk_sig} - \text{osc_sig}\} \right|^2 \quad (87)$$

Provided the simulation sampling rate f_s , the indices $[0, n_steps/2-1]$ of the FFT and consequently `psd` correspond to frequencies $[0, \text{fbin} \cdot (n_steps/2-1)]$, where $\text{fbin} = f_s/n_steps$. Slicing the power spectrum data `psd` with indices $[1, \text{fbin} \cdot (n_steps/2-1)]$ will yield the single side band spectrum of the oscillator, with the corresponding offset frequency of each index k being $\Delta f_k \cdot \text{fbin}$. Thus:

$$\mathcal{L}(\Delta f) = \text{psd}[\text{round}(\Delta f / \text{fbin})] \quad (88)$$

4.8 Monte-Carlo sampling

The simulation code implemented uses a Python dictionary containing the simulation parameters and the corresponding parameters for which the simulation engine should simulate the PLL for. This format makes the introduction of Monte-Carlo sampling into the simulator straightforward. This can be implemented utilizing a dictionary with the nominal simulation configuration, and then a second dictionary to define the parameters to be varied along with the corresponding parameter variance. Given a sample size of N for the Monte-Carlo simulation, a loop is implemented which creates a new simulation configuration dictionary each loop iteration with stochastically sampled values from a normal distribution based on the provided nominal configuration and variance dictionaries. That unique configuration dictionary instance is used to spawn a PLL simulation, and is stored. After N iterations, N sets of data are created with varied parameters.

5 Loop filter optimization

The loop filter optimization engine implemented utilizes constrained optimization to minimize total phase noise of the PLL subject to lock time constraints. The optimizer is limited to optimizing for a loop filter in the form of 89, having parameters K_i, ω_p, ω_z . Following the theory of section 2.2, the PLL will have open loop and normalized closed loop transfer functions $L(s)$ and $\hat{T}(s)$ in 90 and 91 respectively. Computationally fast methods utilizing the continuous closed-loop PLL approximation $\hat{T}(s)$ to estimate PLL settling time and phase noise are implemented as cost functions for the optimizer.

$$H_{LF}(s) = \frac{K_i \left(\frac{s}{\omega_z} + 1 \right)}{s \left(\frac{s}{\omega_p} + 1 \right)} \quad (89)$$

$$L(s) = \frac{K \left(\frac{s}{\omega_z} + 1 \right)}{s^2 \left(\frac{s}{\omega_p} + 1 \right)} \quad (90)$$

$$\hat{T}(s) = \frac{L(s)}{1 + L(s)} = \frac{K \left(\frac{s}{\omega_z} + 1 \right)}{s^2 \left(\frac{s}{\omega_p} + 1 \right)} \quad (91)$$

Filter optimization follows the following sequency:

1. Minimize integrated phase noise with $\hat{T}(s)$ definition of closed loop behavior. Yields optimal $\{K, \omega_p, \omega_z\}$.
2. Translate optimal parameters to prototype loop filter parameters, perform continuous to discrete time filter conversion.
3. Optimize fixed point resolution of digital loop filter implementation for finite word effects.

The following sections detail the optimizer methods implemented.

5.1 Fast estimation of PLL settling time

Based on the continuous model approximation of ADPLL dynamics, the PLL closed loop phase transfer function $\hat{T}(s)$ is defined as a rational function of two polynomial functions of s , with P poles and Z zeros. Such a transfer function is computationally represented with arrays A and B , containing the denominator and numerator polynomial coefficients.

$$\hat{T}(s) = \frac{\sum_{j=0}^Z b_j s^j}{\sum_{k=0}^P a_k s^k} \quad (92)$$

An estimate of the step response settling time of $T(s)$ can be by utilizing its representation in state space. This is given in 93, with input vector $U(s)$, state vector $\mathbf{X}(s)$, and output $Y(s)$. The state-space representation from a s -domain transfer function can be quickly solved computationally with available signal processing packages such as `scipy.signal` given the coefficient arrays A and B .

$$s\mathbf{X}(s) = \mathbf{A}\mathbf{X}(s) + \mathbf{B}U(s) \quad (93)$$

$$Y(s) = \mathbf{C}\mathbf{X}(s) + \mathbf{D}U(s) \quad (94)$$

The set of k eigenvalues $\{\lambda_1, \dots, \lambda_N\}$ corresponding to poles for the system are found as the roots of 95 [1].

$$|\mathbf{A} - \lambda\mathbf{I}| = 0 \quad (95)$$

Imposing the constraint of number of poles $P >$ number of zeros Z , the system $T(s)$ may be represented via partial fraction decomposition using the poles from the eigenvalues of state matrix \mathbf{A} $\{\lambda_1, \dots, \lambda_N\}$:

$$T(s) = \sum_{k=1}^P \frac{c_k}{s - \lambda_k} \quad (96)$$

Inverse Laplace transformation shows the step response of the system will be a sum of exponentials:

$$y(t) = c_1 e^{\lambda_1 t} + \dots + c_k e^{\lambda_k t} \quad (97)$$

The dynamics of the step response are governed by the exponential components of $y(t)$. If $\{\lambda_1, \dots, \lambda_N\} \in \mathbb{C}$ where $\lambda_k = 1/\tau_k + j\omega_K$, the real portion of each λ_k will describe the transient behavior of each exponential, having time constant τ_k . The long term settling of $y(t)$ will be dominated by the exponential with the largest τ_k , i.e. the dominant pole of the system. This estimate of settling time uses the dominant pole τ_k as a heuristic estimate for overall time constant of the system, τ . Finally, settling time t_s can be considered as the time interval required for the signal to drop within a tolerance band $\pm\delta_{tol}y(\infty)$ about the final value $y(\infty)$. Thus:

$$t_s = \tau \ln(\delta_{tol}) = \frac{\ln(\delta_{tol})}{\min(|\Re(\{\lambda_1, \dots, \lambda_k\})|)} \quad (98)$$

This settling time estimate is computationally fast, as it requires only (a) computation of state matrix \mathbf{A} , (b) computation of the eigenvalues of \mathbf{A} , and (c) computation of settling time from the eigenvalue with minimum real component.

5.2 Estimation of PLL phase noise

It is assumed here that [DISCUSSION EXPLAINS WHY...] the dominant output-referred phase noise contributions of the PLL are due to the DCO thermal noise and TDC quantization. If S_{TDC} and S_{DCO} are the PLL output-referred noise PSD respectively for the TDC and DCO noise sources from section 2.3, the total PLL output noise PSD $S_{\Sigma}(f)$ is estimated as 99. N is the PLL divider modulus.

$$S_{\Sigma}(f) = S_{\Phi_{n_{TDC,out}}}(f) + S_{\Phi_{n_{DCO,out}}}(f) \quad (99)$$

$$= \frac{1}{12f_{ref}} \left| 2\pi \frac{N}{M} \hat{T}(f) \right|^2 + \frac{S_{0\Phi_{n_{DCO}}}}{f^2} \left| 1 - \hat{T}(f) \right|^2 \quad (100)$$

Given a bandwidth of interest Δf (i.e. baseband bandwidth for radio applications), the total integrated phase noise power is:

$$P_{\phi noise} = 2 \int_0^{\Delta f} S_{\Sigma}(f) df \quad (101)$$

This can be computation solved for a grid of K values in the interval Δf , where each point represents a frequency bin $f_{bin} = \Delta f/K$. Therefore this estimate is implemented as such:

$$\hat{P}_{\phi noise} = 2 \sum_{k=0}^{K-1} S_{\Sigma}(kf_{bin}) f_{bin} \quad (102)$$

5.3 Loop filter optimization algorithm

The optimization algorithm in use is predicated on a fixed form for the filter being design, as in 89, and consequently known and fixed open and closed loop transfer function forms. The prototype loop filter design in this work contains a tunable pole ω_p , a tunable zero ω_z and a gain parameter K . To allow the phase noise minimization and the constraint on maximum lock time to both have an impact in the optimization, the optimization is implemented with two nested levels. There is there is a lower level optimizer which will minimize phase noise given a fixed target for settling time. The higher level optimizer applies a constrained search for settling time, utilizing the lower level optimizer, that results in minimum phase noise.

Level A - Minimize phase noise for fixed settling time.

- Minimize phase noise while maintaining fixed settling time $= t_s$.
- **Solution:** use two steps per iteration until satisfactorily converged:
 1. Minimize phase noise using pole/zeros locations (gradient descent).
 2. Tune K such that settling time $= t_s$ (golden section search).

Level B - Optimize settling time given constraints.

- Use golden section search to find optimal constrained settling time that has minimal phase noise using method from level A as cost function.

5.4 Loop filter optimization - finite word effects

Once a filter design has been optimized in the continuous domain following section 5.3, second order optimization is carried out to ensure the digitized, discrete implementation performs as expected in the presence of finite word effects. The optimized digital implementation provided here utilized fixed-point words for equal resolution throughout the datapath. The implemented second order optimization considers both the effect of loop filter quantization noise and transfer function error.

Loop filter quantization noise optimization

6 Discussion and results

- Discuss choices made in simulator
 - Deficiencies, advantages, why they were made
 - Phase noise/lock time analysis
 - Analysis - monte-carlo variation to analyze stability/lock time
 - purpose: to validate filter design
- Filter structure choice - PI with added pole. Why is this best (low complexity, no phase error)
- Why only phase random walk in oscillator phase noise
- Why direct type I implementation
- Discuss choices made in loop filter designer/optimizer
 - Why only optimize for TDC/DCO phase noise initially - (other noise sources are easier to reduce below the limits of these two). Flicker noise ignore due to time resolution limitations, expectation that reference flicker, PLL flicker components as reference flicker with be multiplied by N at output.
 - Plot showing BW vs noise components, motivates optimization approach. PN min when TDC and DCO components roughly equal.
 - Discuss why ref flicker noise doesn't matter (it can't be altered by PLL so it doesn't matter for optimization)
 - Optimizer approach: minimization of phase noise constrained by lock time (BFGS optimizer)
 - Second order optimization of filter design for data representation precision with discrete time considerations (first order design is with approximations from continuous PLL model). Discretized LF noise via simulation with input noise

- Recommendations for divider noise limit
- Design verification
- State of art comparison
 - Compare to state of art/existing frameworks?
 - Existing optimization approaches: second order PLL [6]
 - What are improvements made here?
 - Perrot's pre-existing work: general purpose simulation architecture, doesn't directly handle optimization for integer-N, especially in heavily quantized case
- Design example - compare to existing
 - Design 2.4G PLL for WuRx, show results from process
 - Repeat in CPPsim, compare results?
 - Explain advantage of this framework based on exercise
- Discuss limitations and considerations for use of framework
 - Models are not accurate for frequencies near or greater than reference frequency???
 - Sampling rate recommendations (high oversampling)
 - Minimum choice of TDC resolution, constraints for divider jitter,
 - Optimizer needs poles/zeros

Recommendations for maximum divider jitter, loop filter resolution

6.1 Divider noise constraint

Output referred phase noise PSD of TDC:

$$S_{\Phi_{nTDC,out}} = \frac{1}{12f_{ref}} \left| 2\pi \frac{N}{M} G(f) \right|^2 \quad (103)$$

Output referred phase noise PSD of divider:

$$S_{\Phi_{n_{div},out}} = f_{ref} |2\pi N \sigma_{tn_{div}} G(f)|^2 \quad (104)$$

The output-referred phase noise for the TDC and divider have the same frequency dependence. So by setting $S_{\Phi_{n_{div},out}} < S_{\Phi_{nTDC,out}}$, a constraint to force PLL output divider less than TDC noise can be found:

$$\sigma_{tn_{div}} < \frac{1}{Mf_{ref}} = \Delta t_{stepTDC} \quad (105)$$

Must simply ensure that jitter of divider is much less than TDC resolution, which is a reasonable demand. Thus, it is reasonable to ignore divider noise in the phase noise

optimization if divider noise can reasonably be made insignificant in the overall output phase noise.

6.2 Example exercise

Use WuRx design specs to motivate design example... put updated/better definition of specs relative to design example

Parameter	Value	Unit	Notes
Frequency	2.4-2.4835	GHz	2.4G ISM Band
Ref. frequency	16	MHz	Yields 6 channels
Power	≤ 100	μW	
Residual FM	≤ 107	kHz_{RMS}	$\text{BER} \leq 1\text{e-}2$, $f_{dev} = \pm 250 \text{ KHz}$
Initial Lock Time	≤ 50	μs	Upon cold start
Re-lock Time	≤ 5	μs	Coming out of standby
Bandwidth	100	kHz	(nominally), tunable

Table 1: System-level specifications

Parameter	Value	Unit	Notes
DCO LSB Resolution	≤ 50	kHz	Determined from quantization noise.
DCO DNL	< 1	LSB	Ensures monotonicity
TDC Resolution	≤ 3.8	ns	
TDC Resolution (bits)	≥ 4.03	bits	

Table 2: Component-level specifications.

7 Conclusion

Extend to fractional-N. Loop filter design will be the same, difference is divider model.

8 Baseband phase noise in radio with PLL

This doesn't have a home yet, perhaps appendices... will be relevant for BER estimation for radio system (will be referenced in discussion)

8.1 Modulated Signal

A generalized FSK/PSK modulated signal $x_s(t)$ can be written in the following with phase trajectory $\phi_s(t)$. $\phi_s(t)$ is composed of a modulation component $\phi_m(t)$ and carrier component $\omega_c t$.

$$x_s(t) = A_s \cos(\phi_s(t)) = A_s \cos(\phi_m(t) + \omega_c t) \quad (106)$$

8.2 Local oscillator - noisy PLL

A noisy PLL can be realized as $x_{lo}(t)$ with phase trajectory $\phi_{lo}(t)$. $\phi_{lo}(t)$ is comprised of a phase noise component $\phi_n(t)$ and an oscillation $\omega_{lo} t$.

$$x_{lo}(t) = A_{lo} \cos(\phi_{lo}(t)) = A_{lo} \cos(\phi_n(t) + \omega_{lo} t) \quad (107)$$

8.3 Baseband phase noise

The signal in the baseband, $x_{bb}(t)$, is given by mixing $x_s(t)$ with the LO $x_{lo}(t)$. For analysis of the baseband phase noise, zero-IF ($\omega_c = \omega_{lo}$) is considered. Thus:

$$x_{bb}(t) = A_s \cos(\phi_m(t) + \omega_c t) \cdot A_{lo} \cos(\phi_n(t) + \omega_{lo} t) \quad (108)$$

$$= \frac{1}{2} A_s A_{lo} [\cos(2\omega_{lo} t + \phi_m(t) + \phi_n(t)) + \cos(\phi_m(t) - \phi_n(t))] \quad (109)$$

The $2\omega_{lo} t$ component is assumed to be rejected due to limited mixer bandwidth. Thus the baseband signal is now:

$$x_{bb}(t) = A_s \cos(\phi_m(t) + \omega_c t) \cdot A_{lo} \cos(\phi_n(t) + \omega_{lo} t) \quad (110)$$

$$= \frac{1}{2} A_s A_{lo} [\cos(\phi_m(t) - \phi_n(t))] = \frac{1}{4} A_s A_{lo} [e^{j\phi_m(t)} e^{-j\phi_n(t)} + e^{-j\phi_m(t)} e^{j\phi_n(t)}] \quad (111)$$

The phase noise is presumed to be comprised of random phase and frequency walk, such that $\langle \phi_n(t) \rangle = 0$. Also, the phase noise is presumed to be small in amplitude, such that $\phi_n(t) \ll 1$, so a Taylor polynomial-based approximation of $e^{-j\phi_n(t)} = 1 - j\phi_n(t)$ can be made. Accordingly :

$$x_{bb}(t) \approx \frac{1}{4} A_s A_{lo} [e^{j\phi_m(t)} (1 - j\phi_n(t)) + e^{-j\phi_m(t)} (1 + j\phi_n(t))] \quad (112)$$

$$= \frac{1}{4} A_s A_{lo} [\cos(\phi_m(t)) + \phi_n(t) \sin(\phi_m(t))] \quad (113)$$

The above can be treated as a signal component $m(t) = \cos(\phi_m(t))$, and a noise component $n(t) = \phi_n(t) \sin(\phi_m(t))$. The Fourier transform of the noise component can be considered:

$$N(f) = \mathcal{F}\{\phi_n(t) \sin(\phi_m(t))\} = \Phi_n(f) * \mathcal{F}\{-\cos(\phi_m(t) + \pi/2)\} \quad (114)$$

$$= -j\Phi_n(f) * \mathcal{F}\{\cos(\phi_m(t))\} \quad (115)$$

The signal and noise power spectral densities are therefore approximately:

$$S_{MM} = |M(f)|^2 = |\mathcal{F}\{\cos(\phi_m(t))\}|^2 \quad (116)$$

$$S_{NN} = |N(f)|^2 = |\Phi_n(f) * \mathcal{F}\{\cos(\phi_m(t))\}|^2 \quad (117)$$

The in-band noise and signal power of these components can be easily computed via integration:

$$P_x = \int_{-\Delta f/2}^{+\Delta f/2} S_{XX} df \quad (118)$$

SNR is therefore the ratio of P_M/P_N within a bandwidth of interest Δf , which is straightforward to determine computationally for arbitrary PLL phase noise and modulation spectral densities.

References

- [1] R. Brockett. “Poles, zeros, and feedback: State space interpretation”. In: *IEEE Transactions on Automatic Control* 10.2 (1965), pp. 129–135. DOI: [10.1109/tac.1965.1098118](https://doi.org/10.1109/tac.1965.1098118).
- [2] F. Gardner. “Charge-Pump Phase-Lock Loops”. In: *IEEE Transactions on Communications* 28.11 (Nov. 1980), pp. 1849–1858. DOI: [10.1109/tcom.1980.1094619](https://doi.org/10.1109/tcom.1980.1094619).
- [3] M.h. Perrott, M.d. Trott, and C.g. Sodini. “A modeling approach for Sigma-Delta fractional-N frequency synthesizers allowing straightforward noise analysis”. In: *IEEE Journal of Solid-State Circuits* 37.8 (2002), pp. 1028–1038. DOI: [10.1109/jssc.2002.800925](https://doi.org/10.1109/jssc.2002.800925).
- [4] Behzad Razavi. *Design of analog CMOS integrated circuits*. McGraw-Hill Education, 2017.
- [5] Behzad Razavi. “Design of monolithic phase-locked loops and clock recovery circuitsDa tutorial”. In: 1996.
- [6] A. Spalvieri. “Optimal Loop Filter of the Discrete-time PLL in the Presence of Phase Noise”. In: *11th IEEE Symposium on Computers and Communications (ISCC06)* (2006). DOI: [10.1109/iscc.2006.115](https://doi.org/10.1109/iscc.2006.115).
- [7] V. Vannicola and P. Varshney. “Spectral Dispersion of Modulated Signals Due to Oscillator Phase Instability: White and Random Walk Phase Model”. In: *IEEE Transactions on Communications* 31.7 (1983), pp. 886–895. DOI: [10.1109/tcom.1983.1095902](https://doi.org/10.1109/tcom.1983.1095902).

A Appendix - Schedule

remove

Week Number	Dates	Tasks	Outcomes
36	2.9 - 8.9	Review PLL Design	Refreshed Knowledge
37	9.9 - 15.9	Modeling/simulation (set up)	–
38	16.9 - 22.9	Modeling/simulation	TDC/DCO Requirements
39	23.9 - 29.9	Modeling/simulation	Loop Filter/Digital Algorithms
40	30.9 - 6.10	Modeling/simulation	Loop filter , Ideal implementation in Cadence
41	7.10 - 13.10	Circuit Research	DCO/Divider topologies
42	14.10 - 20.10	Circuit Research	TDC/other topologies
43	21.10 - 27.10	Circuit Implementation	Digital logic (schematic)
44	28.10 - 3.11	Circuit Implementation	DCO (schematic)
45	4.11 - 10.11	Circuit Implementation	Divider/other (schematic)
46	11.11 - 17.11	Circuit Implementation (TDC)	
47	18.11 - 24.11	Circuit Implementation (TDC)	TDC (schematic)
48	25.11 - 1.12	Full Circuit testing	Testbenches, find bugs, design fixes
49	2.12 - 8.12	Full Circuit testing	Design Fixes/iteration
50	9.12 - 15.12	–	–

Legend: **Done** **Current** **Revised**